Synthesis, structure, and luminescence properties of sodium and ytterbium complexes with 2-(benzothiazol-2-yl)selenophenolate ligands*

V. A. Ilichev,[a] T. V. Balashova,[a] S. K. Polyakova,[a] A. F. Rogozhin,[a] D. S. Kolybalov,[b,c] D. A. Bashirov,[b] S. N. Konchenko,[b] A. N. Yablonskiy,[d] R. V. Rumyantcev,[a] G. K. Fukin,[a] and M. N. Bochkarev[a]★

[a]*G. A. Razuvaev Institute of Organometallic Chemistry, Russian Academy of Sciences, 49 ul. Tropinina, 603950 Nizhny Novgorod, Russian Federation. E-mail: ilichev@iomc.ras.ru*
[b]*Nikolaev Institute of Inorganic Chemistry, Siberian Branch of the Russian Academy of Sciences, 3 prosp. Akad. Lavrentieva, 630090 Novosibirsk, Russian Federation*
[c]*Novosibirsk State University, 2 ul. Pirogova, 630090 Novosibirsk, Russian Federation*
[d]*Institute for Physics of Microstructures, Russian Academy of Sciences, 7 ul. Akademicheskaya, Afonino, Kstovo district, 603950 Nizhny Novgorod region, Russian Federation*

With the aim of designing new heteroorganic ligands capable of sensitizing the metal-centered photoluminescence (PL) of Yb^{III} through the redox mechanism, a new diselenide, 2,2′-(diseleno-2,1-diphenylene)bis[benzothiazole] ($(SeSN)_2$, **1**), was synthesized and structurally characterized. The selenophenolate complexes $Na(SeSN)(DME)_2$ (**2**) and $Yb(SeSN)_3 \cdot 0.5$ THF (**3**) were synthesized by the reactions of diselenide **1** with Na and Yb metals in liquid ammonia. Complex **2** showed intense PL at 77 K in a DME solution, which appears as a broad band with a maximum at 575 nm assigned to the phosphorescence of the organoselenide ligand. In the crystalline state, ytterbium complex **3**, which was isolated and structurally characterized as an adduct with THF, exhibited intense metal-centered PL in the 980—1100 nm region. This PL is observed upon direct excitation or upon excitation through SeSN ligands (250—380 nm), as well as through excitation of the ligand-to-metal charge transfer (LMCT) band in the 430—700 nm region. The presence of low-energy LMCT states capable of sensitizing the metal-centered PL of Yb^{III} in complexes with organoselenide ligands is responsible for a significant reduction of the Stokes shift of luminescence and opens up new prospects for the development of lanthanide-containing infrared luminophores exhibiting luminescence under long-wavelength excitation.

Key words: ytterbium, photoluminescence, energy transfer, organoselenium compounds, ligand-to-metal charge transfer, infrared luminescence.

The characteristic narrow-band luminescence of lanthanide(III) ions is used in many areas of modern science and engineering, in particular, in bioimaging agents,[1] organic light-emitting diodes,[2] up-conversion materials,[3] and so on.[4] The unique luminescence properties of lanthanide ions are related to *f—f* transitions. Apart from obvious advantages, *f—f* luminescence has a number of drawbacks, the main of which are the forbidden nature of *f—f* transitions and, as a consequence, low extinction coefficients.[5] The problem of insufficient absorption of lanthanides can be addressed by the binding of ions to form complexes with organic ligands having intense absorption, which can also efficiently transfer the excitation energy to lanthanide ions. These ligands, referred to as "antenna ligands", generally transfer excitation energy to resonance 4*f* levels of lanthanides from the triplet level *via* the Förster or Dexter mechanisms.[6] Besides, in the case of ytterbium, the ligand-to-metal excitation energy transfer can occur through an alternative non-resonant mechanism. As demonstrated previously,[7,8] trivalent ytterbium can be reduced with excited ligands to the divalent state and oxidized to the trivalent state through the relaxation, resulting in the excited 4*f* configuration of the ion. The main advantage of the redox excitation pathway of lanthanides over the resonant pathway is that it does not require the selection of ligands for the formation of the optimal energy gap between the triplet level of the ligands and the resonance level of the metal. In this case, ligands showing strong reducing properties should be used for the synthesis of efficient luminescent complexes. Previously, the non-resonant mechanism of PL excitation of Yb^{III} was

* Dedicated to Corresponding Member of the Russian Academy of Sciences A. A. Trifonov on the occasion of his 60th birthday.

Published in Russian in *Izvestiya Akademii Nauk. Seriya Khimicheskaya,* No. 2, pp. 298—305, February, 2022.
1066-5285/22/7102-0298

proposed for ytterbium complexes with thiolate ligands, in particular with 2-mercaptobenzothiazole[9] and benzox(thi)azolyl-substituted thiophenols.[10] Besides, ytterbium complexes with these ligands possess low-energy ligand-to-metal charge transfer (LMCT) states, which leads to the enhancement of the efficiency of the excitation energy transfer to the ytterbium ion. Selenols proved to be stronger reducing agents compared to the related thiols and, consequently, they can be considered as promising antenna ligands for non-resonant PL sensitization of Yb^{III}. However, pentafluroselenophenol is currently the only known selenolate ligand capable of sensitizing the metal-centered PL of lanthanides.[11]

The goals of this study were to extend the range of selenolate antenna ligands and investigate the specific features of the excitation energy transfer in their complexes with ytterbium. For this purpose, we synthesized a new diselenide, 2,2′-(diseleno-2,1-diphenylene)bis[benzothiazole] (**1**), and used it as the starting compound to prepare sodium and ytterbium complexes with 2-(benzothiazol-2-yl)selenophenolate (SeSN) ligands. The latter are selenolate analogs of 2-(benzothiazol-2-yl)thiophenolate ligands, which exhibit efficient energy transfer from ligands to ytterbium in the complex and also display high intensity of metal-centered photo- and electroluminescence.[10]

Results and Discussion

Target diselenide **1** was synthesized by the condensation of 2,2′-diselenobis(benzoic acid) with *o*-aminothiophenol in polyphosphoric acid (PPA) according to Scheme 1. The product was isolated as a beige powder and was characterized by ^{1}H NMR spectroscopy and elemental analysis. Single crystals of **1** suitable for X-ray diffraction were obtained by the recrystallization from tetrahydrofuran.

The molecular structure of **1** (Fig. 1) is similar to that of the disulfide derivative prepared previously.[12] Two 2-(benzothiazol-2′-yl)selenophenolate (SeSN) moieties are nearly perpendicular to each other. The dihedral angle between the planes of these moieties is 88.08°. The dihedral angle between the 2-benzothiazol-2′-yl and selenophenolate moieties is 8.95° for Se(1)S(1)N(1) and 8.49° for Se(2)S(2)N(2). The Se(1)—Se(2) distance in **1** is 2.3641(7) Å (Table 1), which is in good agreement with the corresponding values for the related compounds.[13,14]

Scheme 1

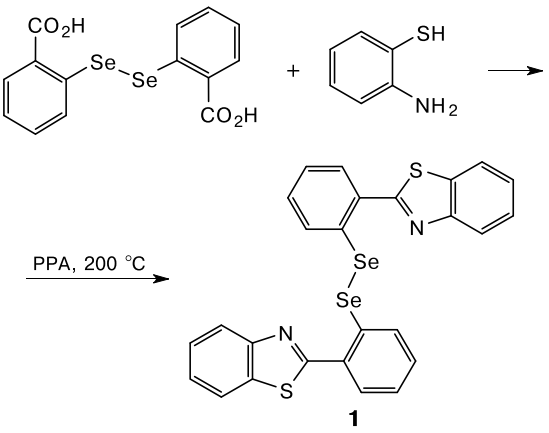

In the crystal, molecules **1** form dimers through weak π...π interactions (Fig. 2). The dihedral angle between the planes of the C_6 aromatic systems of adjacent molecules **1** is 8.62°. The planes of the five-membered heterocycles are strictly parallel to each other and are packed face-to-face. The distance between the centroids of the five-membered heterocycles is 3.76 Å, which is indicative of the presence of an intermolecular interaction. The angle between the normal of one C_6 aromatic system to the plane of another C_6 ring and the vector of the centroids of these rings is 24.47°. The distance between the centroids of the rings of the adjacent molecules is 4.08 Å. These geometric characteristics are only slightly larger than the geometric criterion for the existence of an intermolecular π...π interaction (3.80 Å).[15]

Diselenide **1** was used in the synthesis of the sodium and ytterbium complexes (Scheme 2). The reductive cleavage of the Se—Se bond occurs upon the addition of disel-

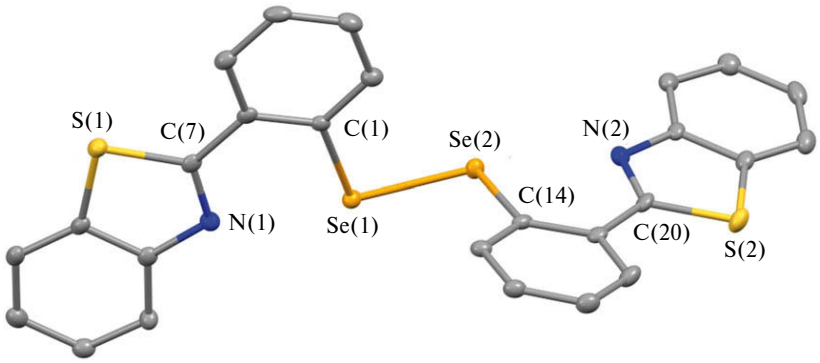

Fig. 1. Molecular structure of diselenide **1** with displacement ellipsoids drawn at the 30% probability level. Hydrogen atoms are omitted for clarity.

Table 1. Selected bond lengths (*d*) and bond angles (ω) of compound **1**

Bond	*d*/Å	Bond	*d*/Å	Angle	ω/deg
Se(1)—C(1)	1.960(3)	S(2)—C(20)	1.762(4)	C(1)—Se(1)—Se(2)	102.57(12)
Se(1)—Se(2)	2.3641(7)	N(1)—C(7)	1.316(4)	C(14)—Se(2)—Se(1)	101.23(13)
Se(2)—C(14)	1.956(4)	N(1)—C(13)	1.401(5)	C(8)—S(1)—C(7)	89.52(19)
S(1)—C(8)	1.755(4)	N(2)—C(20)	1.314(5)	C(26)—S(2)—C(20)	88.7(2)
S(1)—C(7)	1.766(4)	N(2)—C(21)	1.397(5)	C(7)—N(1)—C(13)	110.2(4)
S(2)—C(26)	1.742(4)			C(20)—N(2)—C(21)	111.0(4)

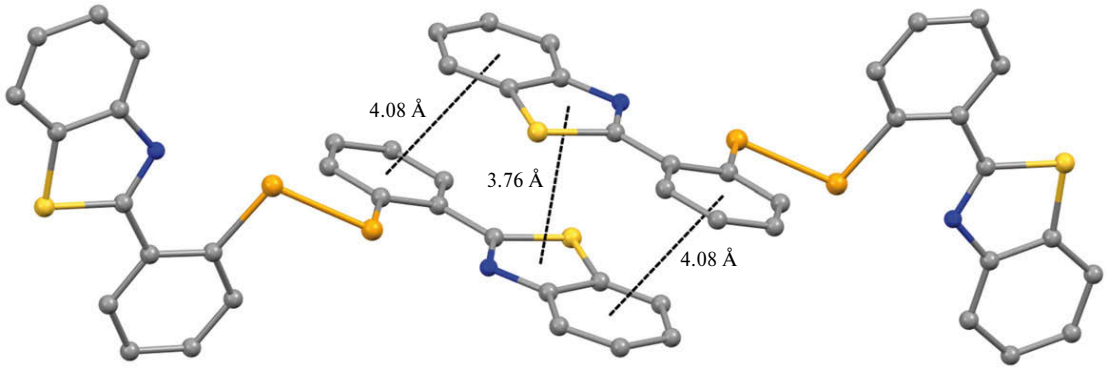

Fig. 2. Fragment of the crystal packing of diselenide **1**.

enide **1** to a solution of the corresponding metals in liquid ammonia at 223 K. The complex Na(SeSN)$(DME)_2$ (**2**) was isolated as a yellow-orange powder having a strong unpleasant smell and was characterized by IR and NMR spectroscopy and elemental analysis. The ytterbium complex $Yb(SeSN)_3 \cdot 0.5THF$ (**3**) was recrystallized from a toluene—tetrahydrofuran mixture and was isolated as brown prismatic crystals.

Scheme 2

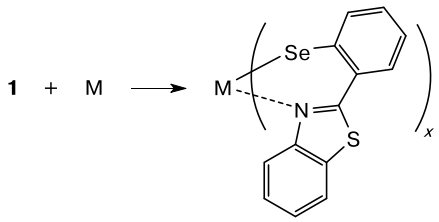

2, 3

2: M = Na, *x* = 1; **3:** M = Yb, *x* = 3

Reagents and conditions: NH_3 (liq), −50 °C.

According to the X-ray diffraction data, complex **3** is a monomer, in which the ytterbium atom is surrounded by three bidentate SeSN ligands (Fig. 3). The ytterbium atom has the coordination number 6, and the coordination environment of ytterbium can be described as a distorted octahedron. This structure is in good agreement with that of the ytterbium thiophenolate derivative published previously.[10] The Yb—N distances of complex **3** (2.426(8)—2.512(17) Å) are characteristic of the Yb—N coordination interactions. The Yb—Se distances (2.67(2)—2.7692(12) Å) (Table 2) are longer than the Yb—S distances (2.6147(10)—

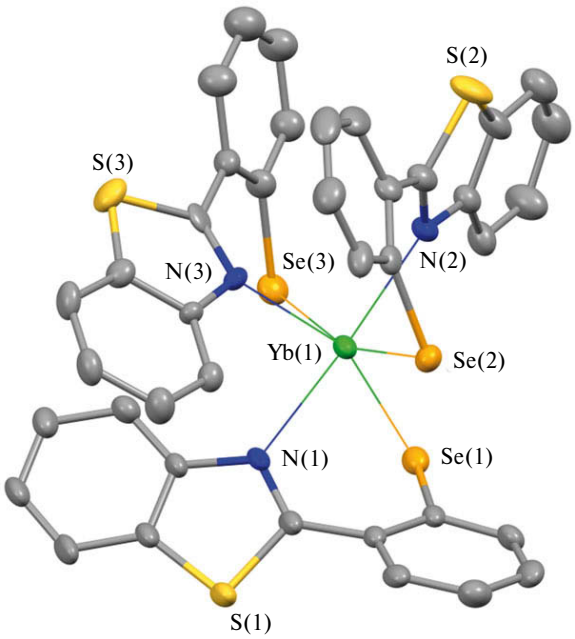

Fig. 3. Molecular structure of complex **3** with displacement ellipsoids drawn at the 30% probability level. Hydrogen atoms are omitted for clarity.

Table 2. Selected bond lengths (*d*) of compound **3**

Bond	*d*/Å	Bond	*d*/Å	Bond	*d*/Å
Yb(1)—N(1)	2.426(8)	Se(2)—C(14)	1.911(11)	N(2)—C(20)	1.319(14)
Yb(1)—N(2)	2.426(8)	S(1)—C(9)	1.729(12)	N(2)—C(21)	1.413(14)
Yb(1)—N(3)	2.512(17)	S(1)—C(7)	1.749(11)	Se(3)—C(27)	1.914(16)
Yb(1)—Se(3)	2.67(2)	S(2)—C(22)	1.711(14)	S(3)—C(34)	1.70(2)
Yb(1)—Se(1)	2.7503(12)	S(2)—C(20)	1.743(11)	S(3)—C(33)	1.754(16)
Yb(1)—Se(2)	2.7692(12)	N(1)—C(7)	1.320(14)	N(3)—C(33)	1.306(18)
Se(1)—C(1)	1.923(12)	N(1)—C(8)	1.408(12)	N(3)—C(35)	1.382(17)

Table 3. Selected bond angles (ω) of compound **3**

Angle	ω/deg	Angle	ω/deg	Angle	ω/deg
N(1)—Yb(1)—N(2)	171.9(3)	N(3)—Yb(1)—Se(3)	83.0(9)	N(1)—Yb(1)—Se(2)	98.6(2)
N(1)—Yb(1)—N(3)	81.4(8)	N(1)—Yb(1)—Se(1)	77.69(19)	N(2)—Yb(1)—Se(2)	76.6(2)
N(2)—Yb(1)—N(3)	92.0(8)	N(2)—Yb(1)—Se(1)	109.5(2)	N(3)—Yb(1)—Se(2)	90.0(9)
N(1)—Yb(1)—Se(3)	96.4(5)	N(3)—Yb(1)—Se(1)	157.2(10)	Se(3)—Yb(1)—Se(2)	162.3(3)
N(2)—Yb(1)—Se(3)	87.4(5)	Se(3)—Yb(1)—Se(1)	90.4(4)	Se(1)—Yb(1)—Se(2)	101.97(4)

2.6413(10) Å) in the thiophenolate derivative.[10] This fact is well consistent with the difference in the van der Waals radii of sulfur (1.8 Å) and selenium (1.9 Å).[16]

As opposed to diselenide **1**, the dihedral angles between the benzothiazolate and selenophenolate moieties in complex **3** vary in the range of 35.58—45.80°.

In the crystal, the adjacent molecules of complex **3** form infinite chains through weak π...π interactions (Fig. 4). The dihedral angle between the planes of the benzothiazole moieties is 7.48°. The distance between the centroids of the five-membered heterocycles is 3.78 Å. The angle between the normal of one heterocycle to the plane of another heterocycle and the vector of the centroids of these rings is 12.90°. The distance between the centroids of the phenyl rings of the ligands of the adjacent molecules is 3.73 Å, and the angle between the normal of one ring to the plane of another ring and the vector of the centroids of these rings is 20.57°. These values are indicative of the presence of intermolecular π...π interactions in complex **3**. Besides, the distance between the centroids of the phenyl rings of the adjacent ligands within one molecule (3.83 Å) is only slightly larger than the geometric criterion for the existence of a π...π interaction.[15]

The absorption spectrum of complex **2** (Fig. 5, *a*) shows intense bands at 250—350 nm assigned to π—π transitions in SeSN ligands. Apart from these bands, there is a less intense absorption band at 400—500 nm, which is responsible for the characteristic yellow-orange color of complex

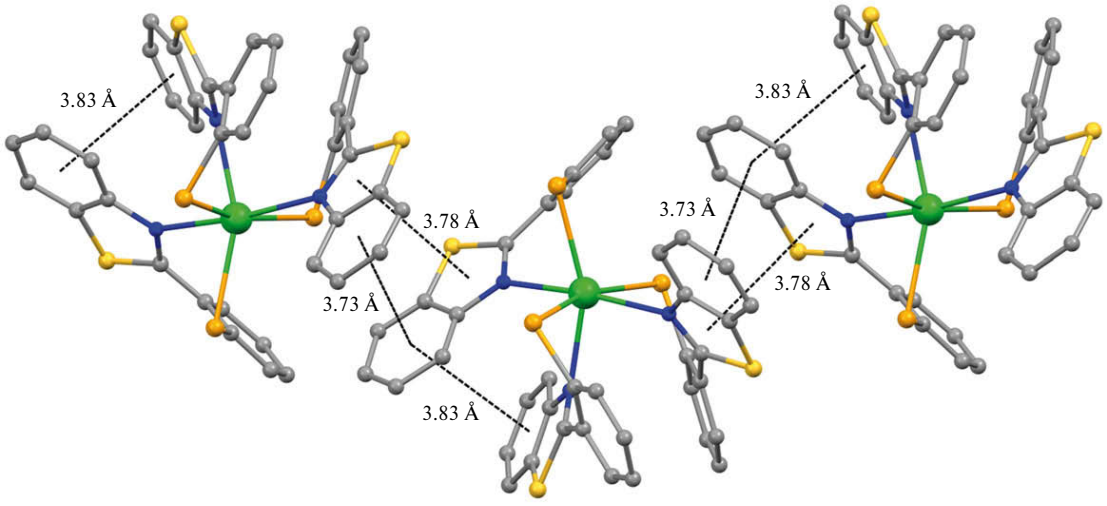

Fig. 4. Fragment of the crystal packing of complex **3**.

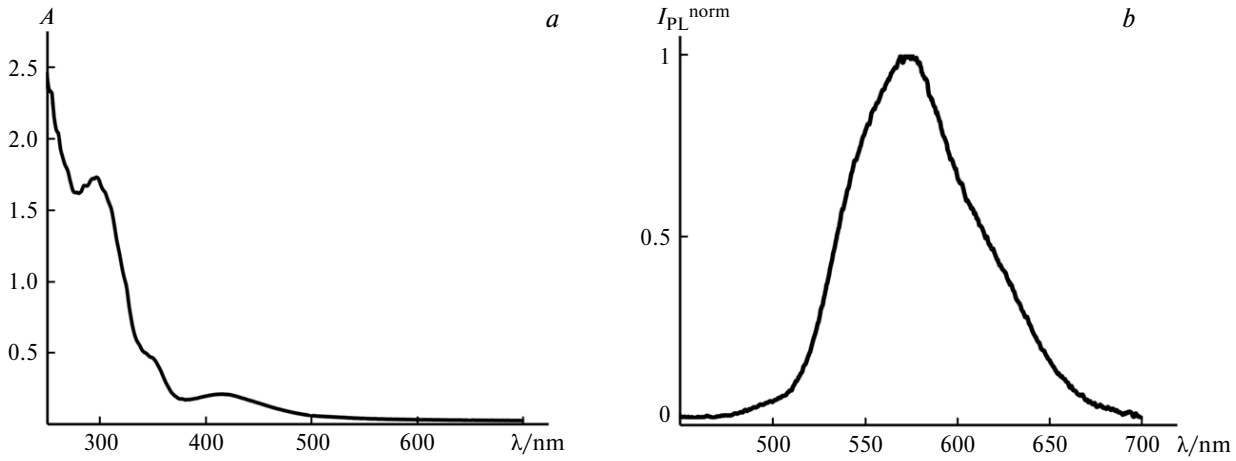

Fig. 5. Absorption spectrum (*a*) and the PL spectrum of complex **2** in DME at 77 K under diode laser excitation at 405 nm (*b*). I_{PL}^{norm} is the normalized fluorescence intensity.

2 and apparently belongs to intraligand charge-transfer absorption. At room temperature, PL was observed for complex **2** neither in the solid state nor in solution under excitation at wavelengths of 250—500 nm. However, at a liquid nitrogen temperature, complex **2** exhibited intense yellow-green PL assigned, apparently, to the phosphorescence of the SeSN ligand with a broad-band maximum at about 575 nm (Fig. 5, *b*). The energy of the triplet level of the SeSN ligand calculated from this spectrum is 19200 cm^{-1}.

The triplet level of the selenophenolate SeSN ligand is somewhat lower in energy compared to those of the related phenolate and thiophenolate ligands.[10] Nevertheless, the energy gap between this level and the sole excited 4*f* state of the Yb^{3+} ion, $^2F_{5/2}$, is about 9000 cm^{-1}. According to Latva´s rule,[4] this fully excludes the possibility of energy transfer between these states in complex **3**. Nevertheless, complex **3** exhibits not only metal-centered PL of the ytterbium ion under direct excitation of the $^2F_{7/2} \rightarrow {}^2F_{5/2}$ transition of the ion (Fig. 6, *a*) but also much more intense luminescence under excitation through the ligand levels by Nd:YAG laser radiation with a wavelength of 355 nm, which is indicative of the non-resonant mechanism of SeSN ligand-sensitized ytterbium luminescence.

The mechanism of sensitization of ytterbium PL in complex **3** is apparently similar to that described previously for the ytterbium complex with the thiolate analog of the SeSN ligand.[10] The LMCT states play a special role in this mechanism. These states have a relatively low energy and can be determined by analyzing the PL excitation spectra in the visible region. Figure 7 presents the spectrum of crystals of complex **3** recorded under PL excitation using an optical parametric oscillator (OPO). As can be

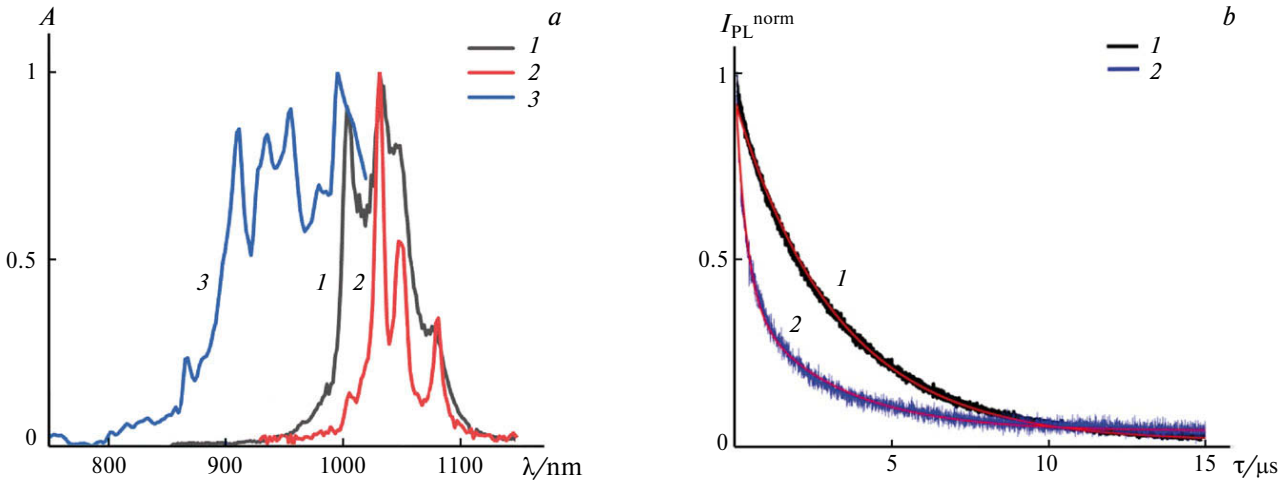

Fig. 6. Photoluminescence spectra (*1*, *2*) and the PL excitation spectrum at a wavelength of 1036 nm (*3*) of complex **3** at 293 (*1*) and 77 K (*2*) in the near-IR region (*a*); the kinetic dependences of the PL intensity of complex **3** at a wavelength of 1036 nm at 293 (*1*) and 77 K (*2*) and their fitting curves (*b*).

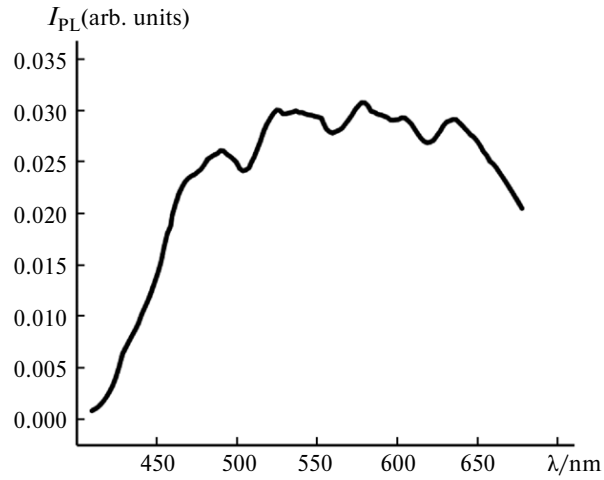

Fig. 7. Photoluminescence excitation spectrum of the crystals of complex **3** in the visible region under irradiation at λ = 1036 nm.

seen in Fig. 7, the metal-centered PL of Yb^{3+} can be excited with radiation in the visible region at a wavelength of 430—678 nm (the red edge of the PL excitation spectrum is limited by the performance characteristics of the OPO used). The band observed in the PL excitation spectrum apparently belongs to the transition from the ground state to the LMCT state of complex **3** and is responsible for the brown color of its crystals. It is worth noting that in this case, the energy of the LMCT state is much lower compared to that in the related ytterbium complex based on thiophenolate ligands.[10] This is apparently due to the higher reducing ability of selenophenolate compounds compared to the corresponding thiophenolate derivatives. The consequence is the reduction of the Stokes shift and the possibility of using the red spectral region to pump Yb^{3+} excitation in complexes without an extension of the π-electron conjugated system of the ligand. The latter fact is important in view of the possible medical and biological applications of this compound because the red and near-IR radiation falls within the biological tissue transparency window.

Let us consider the changes in the PL properties of complex **3** as the sample is cooled from the room temperature to the liquid nitrogen temperature. At 77 K, the Starks levels are better resolved; besides, the intensity redistribution is observed. This effect was found previously for the ytterbium complex with 2-mercaptobenzothiazolate ligands.[9] It can be related to the presence of one disordered SeSN ligand in complex **3**, which can occupy a strictly defined position in the molecule at 77 K. Apart from the spectral changes, kinetic changes in PL occur in complex **3** with decreasing temperature. Thus, the intensity of the PL band of ytterbium decreases monoexponentially at 293 K with a lifetime of 3.26 μs, whereas a change to the biexponential dependence occurs at 77 K (Fig. 6, *a*) with lifetimes of 0.35 and 2.89 μs. The contribution of the short exponent is almost two times larger than that of the long exponent. This behavior is not typical of lanthanide complexes. Evidently, new mechanisms of quenching of the excited states of Yb^{3+} appear at a low temperature. The nature of these mechanisms is unclear. Probably, this behavior is influenced by the crystal packing effects, the presence of a disordered ligand, or a change in the electronic structure of the complex with decreasing temperature.

In summary, we synthesized and structurally characterized a new diselenide. This diselenide was used as the starting compound to prepare sodium and ytterbium complexes with selenolate SeSN ligands by the reductive cleavage of the Se—Se bond with metals dissolved in liquid ammonia. The ytterbium complex with three chelating SeSN ligands was characterized by X-ray diffraction. This compound exhibited the intense metal-centered PL of ytterbium in the near-IR region, which can be excited by both soft UV radiation and visible light up to the red region. This specificity is associated with the reducing nature of the selenolate ligand and the non-resonant mechanism of energy transfer from the ligand to the ytterbium ion.

Experimental

All reactions and manipulations with compounds were carried out using the Schlenk technique or under a high-purity argon atmosphere. Dimethoxyethane (DME), toluene, and tetrahydrofuran (THF) were dried over sodium benzophenone ketyl by a standard procedure and were withdrawn *in vacuo* immediately before use. All reagents and solvents were commercially available. Commercial liquid ammonia was dried with sodium metal. 2,2′-Diselenobis(benzoic acid) was synthesized by a known procedure.[17]

The C, H, and N elemental analysis was performed on a Euro EA 3000 elemental analyzer. The ytterbium content was analyzed by complexometric titration. The IR spectra were recorded on a Perkin Elmer 577 spectrometer in the region from 4000 to 450 cm^{-1} as Nujol mulls between KBr plates. The NMR spectra were measured on a Bruker Avance III spectrometer (400 MHz) in C_5D_5N and $CDCl_3$ with Me_4Si as the internal standard. Steady-state PL of solid samples was excited with a 100 mW laser diode (λ = 405 nm) and was recorded in the region from 400 to 1700 nm using OceanOptics USB 2000 and OceanOptics NIR 512 spectrometers operating with the SpectraSuite software. Time-resolved PL spectra of crystals of **3** were measured using laser pulse excitation at the third harmonic of a Spectra-Physics Nd:YAG laser at 355 nm (the pulse duration was ~5 ns). The PL signal was dispersed using a grating Acton-2300 spectrometer and was detected using a cooled InP/InGaAs-based Hamamatsu H10330A-75 PMT in the 900—1500 nm range. The PL excitation spectra of crystals of **3** were measured using a Spectra-Physics MOPO-SL optical parametric oscillator with continuous tuning of the radiation wavelength in the spectral range from 430 to 1100 nm (the pulse repletion frequency was 10 Hz, the pulse duration was ~5 ns). The fitting curves for the lifetime of the excited state of complex **3** were calculated with the Origin program by the equations $y(t) = 0.91027*\exp(t/3.26\ \mu s) + y_0$ and $y(t) = 0.58695*\exp(t/0.35\ \mu s) + 0.3602*\exp(t/2.89\ \mu s) + y_0$ at 293 and 77 K, respectively.

2,2′-(Diseleno-2,1-diphenylene)bis[benzothiazole] (1). 2,2′-Diselenobis(benzoic acid) (0.517 g, 1,3 mmol), *o*-aminothiophenol (300 μm, 2.8 mmol), and polyphosphoric acid (2 mL) were placed in a 7 mL vial. The mixture was heated under magnetic stirring for 6 h (the temperature of the magnetic stirrer was 200 °C). After 6 h, the hot solution was poured into a beaker filled with water (100 mL). The precipitate that formed was filtered off on a porous filter 16 and then washed with successive 10 mL portions of water until neutral pH of the wash solution was achieved. The precipitate was dried, placed in a Soxhlet apparatus, and extracted with dichloromethane (20 mL) overnight. The solvent was removed *in vacuo*, and 2,2′-(diseleno-2,1-diphenylene)-bis[benzothiazole] was obtained in a yield of 0.610 g (80%). Found (%): C, 53.8; H, 2.7; N, 4.6. $C_{26}H_{16}N_2S_2Se_2$. Calculated (%): C, 53.98; H, 2.79; N, 4.84. ^{1}H NMR ($CDCl_3$), δ: 8.16 (d, 1 H, CH_{arom}, J = 8.1 Hz); 8.05 (d, 1 H, CH_{arom}, J = 7.9 Hz); 7.95 (d, 1 H, CH_{arom}, J = 7.9 Hz); 7,87 (d, 1 H, CH_{arom}, J = 7.6 Hz); 7.53 (dd, 1 H, CH_{arom}, J = 7.7 Hz, J = 1.0 Hz); 7.44 (t, 1 H, CH_{arom}, J = 7.7 Hz); 7.32 (dd, 1 H, CH_{arom}, J = 7.4 Hz, J = 1.2 Hz); 7.28 (dd, 1 H, CH_{arom}, J = 7.6 Hz, J = 1.5 Hz).

Sodium 2-(benzo[*d*]thiazol-2-yl)phenylselenolate (2). Sodium metal (23 mg, 1 mmol) was dissolved in liquid ammonia (10 mL) at −50 °C. Diselenide **1** (250 mg, 0.86 mmol) was added to the resulting blue solution under the same conditions, which gave a red-brown solution. Ammonia was removed from this solution by vacuum condensation. The precipitate was dissolved in DME, filtered off, and recrystallized from DME. The yield of the finely crystalline yellow-orange powder was 223 mg (83%). Found (%): C, 51.19; H, 5.68; N, 2.92; S, 10.31. $C_{21}H_{28}NNaO_4SSe$. Calculated (%): C, 51.22; H, 5.73; N, 2.84. IR, ν/cm^{-1}: 1582 m, 1557 w, 1503 m, 1314 m, 1291 w, 1261 w, 1248 w, 1229 m, 1124 m, 1098 m, 1075 m, 1026 m, 964 m, 937 w, 896 w, 842 w, 804 m, 748 s, 711 m, 702 w, 676 w, 644 w, 623 w, 591 w, 551 m. ^{1}H NMR (pyridine-d_5), δ: 8.29 (d, 1 H, CH_{arom}, J = 8.1 Hz); 8.01 (d, 1 H, CH_{arom}, J = 7.9 Hz); 7,60 (d, 1 H, CH_{arom}, J = 7.3 Hz); 7.52 (t, 1 H, CH_{arom}, J = 7.2 Hz); 7.40 (t, 1 H, CH_{arom}, J = 7.3 Hz); 7.26 (dd, 1 H, CH_{arom}, J = 6.8 Hz, J = 1.9 Hz); 7.06—7.15 (m, 2 H, 2 CH_{arom}).

Ytterbium tris[2-(benzo[*d*]thiazol-2-yl)phenylselenolate] (3). Complex **3** was synthesized as described for complex **2** from ytterbium metal (40 mg, 23 mmol) and diselenide **1** (250 mg, 86 mmol). Brown crystals suitable for X-ray diffraction were obtained by the recrystallization of the product from a 1 : 1 toluene—THF mixture. The yield was 144 mg (60%). Found (%): C, 45.69; H, 2.68; N, 3.97; Yb, 16.57. $C_{41}H_{28}N_3O_{0.5}S_3Se_3Yb$.

Table 4. Principal crystallographic data and the X-ray diffraction data collection and structure refinement statistics for complexes **1** and **3**

Parameter	Value	
	1	**3**
Molecular formula	$C_{26}H_{16}N_2S_2Se_2$	$C_{41}H_{28}N_3O_{0.50}S_3Se_3Yb$
M/g mol^{-1}	578.45	1076.76
T/K	100(2)	100(2)
Crystal system	Monoclinic	Monoclinic
Space group	$P2_1/c$	$P2_1/c$
Unit cell parameters		
a/Å	7.7722(9)	20.9256(11)
b/Å	7.7769(9)	11.1861(4)
c/Å	37.487(6)	18.1589(7)
α/deg	90	90
β/deg	90.236(11)	108.613(5)
γ/deg	90	90
V/Å^3	2265.8(5)	4028.2(3)
Z	4	4
d_{calc}/mg m^{-3}	1.696	1.775
μ/mm^{-1}	3.466	5.222
Crystal size/mm	0.15×0.07×0.03	0.40×0.20×0.05
F(000)	1144	2076
θ/deg	3.085—29.998	2.987—29.999
Number of reflections		
collected	13036	77053
unique	6581	11742
R_{int}	0.0591	0.1683
R_1	0.0629	0.0921
wR_2 ($I > 2\sigma(I)$)	0.0929	0.1685
R_1	0.1029	0.1687
wR_2 (based on all reflections)	0.1045	0.1899
S	1.010	1.047
Residual electron density (ρ_{max}/ρ_{min})/e Å^{-3}	0.990/−0.745	2.208/−1.753

Calculated (%): C, 45.73; H, 2.62; N, 3.90; Yb, 16.07. The IR spectrum of complex **3** is similar to the IR spectrum of complex **2**.

X-ray diffraction study of compounds **1** and **3** was performed on an Oxford Xcalibur Eos diffractometer (graphite monochromator, Mo-Kα radiation, φ- and ω-scan techniques, λ = 0.71073 Å). The X-ray intensity data sets were integrated using the CrysAlisPro software package.[18] Absorption corrections were applied with the SCALE3 ABSPACK program. The structures were solved using the dual-space algorithm with the SHELXT program package[19] and refined by the full-matrix least-squares method based on F^2_{hkl} with anisotropic displacement parameters for all nonhydrogen atoms using the SHELXTL program package.[20] Hydrogen atoms were positioned geometrically and refined isotropically using a riding model (U_{iso}(H) = 1.2 U_{eq}(C)). In the crystal structure, there are two molecules of complex **3** per uncoordinated THF molecule. One 2-(benzothiazol-2′-yl)selenophenolate ligand (Se(3)N(3)) in complex **3** is disordered over two positions. In order to obtain adequate geometric and thermal parameters, the disordered moieties were refined using the SAME, SADI, DFIX, EADP, and ISOR constraints. Principal crystallographic data and the X-ray diffraction data collection and structure refinement statistics for compounds **1** and **3** are given in Table 4. The structures were deposited with the Cambridge Crystallographic Data Centre (CCDC 2118587 (**1**)) and 2118588 (**3**)) and are available at ccdc.cam.ac.uk/structures/).

The study was performed within the framework of the state assignment using the equipment of the Center for Collective Use "Analytical Center of the IOMC RAS" with the financial support by the Ministry of Science and Higher Education of the Russian Federation (grant "Ensuring the Development of the Material and Technical Infrastructure of the Centers for Collective Use of Scientific Equipment," agreement number 13.CKP.21.0017).

No human or animal subjects were used in this research.

The authors declare no competing interests.

References

1. Y. Ning, M. Zhu, J.-L. Zhang, *Coord. Chem. Rev.*, 2019, **399**, 213028; DOI: 10.1016/j.ccr.2019.213028.
2. L. Wang, Z. Zhao, C. Wei, H. Wei, Z. Liu, Z. Bian, C. Huang, *Adv. Opt. Mat.*, 2019, **7**; DOI: 10.1002/adom.201801256.
3. Q. Zhang, F. Yang, Z. Xu, M. Chaker, D. Ma, *Nanoscale Horiz.*, 2019, **4**, 579; DOI: 10.1039/c8nh00373d.
4. S. V. Eliseeva, J.-C. G. Bünzli, *Chem. Soc. Rev.*, 2010, **39**, 189; DOI: 10.1039/B905604C.
5. J.-C. G. Bünzli, *Handbook on the Physics and Chemistry of Rare Earths*, 2016, **50**, 141; DOI: 10.1016/bs.hpcre.2016.08.003.
6. E. Nakazawa, in *Phosphor Handbook*, 2nd ed., CRC Press, Boca Raton, 2007, c. 123.
7. W. D. Horrocks Jr., P. J. Bolender, W. D. Smith, R. M. Supkowski, *J. Am. Chem. Soc.*, 1997, **119**, 5972; DOI: 10.1021/JA964421L.
8. A. P. Pushkarev, V. A. Ilichev, T. V. Balashova, D. L. Vorozhtsov, M. E. Burin, D. M. Kuzyaev, G. K. Fukin, B. A. Andreev, D. I. Kryzhkov, A. N. Yablonskiy, M. N. Bochkarev, *Russ. Chem. Bull.*, 2013**, 62**, 392; DOI: 10.1007/s11172-013-0051-z.
9. V. A. Ilichev, A. P. Pushkarev, R. V. Rumyantcev, A. N. Yablonskiy, T. V. Balashova, G. K. Fukin, D. F. Grishin, B. A. Andreev, M. N. Bochkarev, *Phys. Chem. Chem. Phys.*, 2015, **17**, 11000; DOI: 10.1039/C4CP05928J.
10. V. A. Ilichev, A. V. Rozhkov, R. V. Rumyantcev, G. K. Fukin, I. D. Grishin, A. V. Dmitriev, D. A. Lypenko, E. I. Maltsev, A. N. Yablonskiy, B. A. Andreev, M. N. Bochkarev, *Dalton Trans.*, 2017, **46**, 3041; DOI: 10.1039/C6DT04519G.
11. W. Wu, X. Zhang, A. Y. Kornienko, G. A. Kumar, D. Yu, T. J. Emge, R. E. Riman, J. G. Brennan, *Inorg. Chem.*, 2018,
12. E. K. Beloglazkina, A. V. Shimorsky, A. G. Majouga, A. A. Moiseeva, N. V. Zyk, *Russ. Chem. Bull.*, 2007, **56**, 2189; DOI: 10.1007/s11172-007-0344-1.
13. S. Panda, P. Kr. Dutta, G. Ramakrishna, C. M. Ready, S. S. Zade, *J. Organomet. Chem.*, 2012, **717**, 45; DOI: 10.1016/j.jorganchem.2012.07.026.
14. G. Mugesh, A. Panda, H. B. Singh, N. S. Punekar, R. J. Butcher, *Chem. Commun.*, 1998, 2227; DOI: 10.1039/a805941a.
15. C. Janiak, *J. Chem. Soc., Dalton Trans.*, 2000, 3885; DOI: 10.1039/B003010O.
16. S. S. Batsanov, *Russ. J. Inorg. Chem.*, 1991, **36**, 1694. 17.
17. J. He, D. Li, K. Xiong, Y. Ge, H. Jin, G. Zhang, M. Hong, Y. Tian, J. Yin, H. Zeng, *Bioorg. Med. Chem.*, 2012, **20**, 3816; DOI: 10.1016/j.bmc.2012.04.033.
18. *Rigaku Oxford Diffraction. CrysAlis Pro software system, version 1.171.38.46*, Rigaku Corporation, Wroclaw, Poland, 2015.
19. G. M. Sheldrick, *Acta Crystallogr., Sect. A: Found. Adv.*, 2015, **71**, 3; DOI: 10.1107/S2053273314026370.
20. G. M. Sheldrick, *Acta Crystallogr., Sect. C: Struct. Chem.*, 2015, **71**, 3; DOI: 10.1107/S2053229614024218.

Received November 9, 2021;
in revised form November 15, 2021;
accepted November 16, 2021